

# Dynamical Scaling Behavior of Percolation Clusters in Scale-free Networks

F. Jasch, Ch. von Ferber and A. Blumen  
*Theoretische Polymerphysik, Universität Freiburg,*  
*Hermann-Herder-Str. 3, D-79104 Freiburg, Germany*  
 (Dated: November 28, 2018)

In this work we investigate the spectra of Laplacian matrices that determine many dynamic properties of scale-free networks below and at the percolation threshold. We use a replica formalism to develop analytically, based on an integral equation, a systematic way to determine the ensemble averaged eigenvalue spectrum for a general type of tree-like networks. Close to the percolation threshold we find characteristic scaling functions for the density of states  $\rho(\lambda)$  of scale-free networks.  $\rho(\lambda)$  shows characteristic power laws  $\rho(\lambda) \sim \lambda^{\alpha_1}$  or  $\rho(\lambda) \sim \lambda^{\alpha_2}$  for small  $\lambda$ , where  $\alpha_1$  holds below and  $\alpha_2$  at the percolation threshold. In the range where the spectra are accessible from a numerical diagonalization procedure the two methods lead to very similar results.

PACS numbers: 05.50.+q,64.60.Ak,05.40.-a,87.18.Sn

## I. INTRODUCTION

Recent studies of nets, ranging from social networks to power grids and the internet, revealed that in many cases the degree distribution  $p_k$ , i.e. the probability that an arbitrary vertex is connected to exactly  $k$  other vertices, often exhibits a power law, namely that  $p_k \sim k^{-\gamma}$  holds [1, 2]. Networks for which this relation is fulfilled are called *scale-free*; scale-free networks differ from the classical random graphs [3], for which the distribution  $p_k$  is Poissonian, and from small-world-networks [4, 5, 6, 7, 8, 9]. Recent works have clarified that the properties of scale-free networks, in particular percolation, differ markedly from the classical case [1, 2, 10, 11, 12]. It turns out that the asymptotic behavior of  $p_k$  for  $k$  large, the so-called tail of  $p_k$ , which is quantified by  $\gamma$ , is fundamental in differentiating between the distinct classes of behavior: Thus for  $\gamma < 4$  the critical exponents change from the usual values found for classical graphs [12, 13].

Now, the topological properties of a network are reflected in the spectral properties of its connectivity matrix  $\mathbf{C}$ : This matrix is constructed by letting its off-diagonal elements  $C_{ik}$  be 1 if  $i$  and  $j$  are connected or 0 otherwise; moreover, the diagonal elements  $C_{ii}$  of  $\mathbf{C}$  are zero. For scale-free networks it was found that the density of the eigenvalues of  $\mathbf{C}$  has a triangular form with a power-law tail [14, 15, 16]. On the other hand, many problems ranging from the dynamics of randomly branched polymers [19] and the stress relaxation of near critical gels [20], over random resistor-capacitor networks [21] to glassy relaxation dynamics [22], depend on the Laplacian  $\mathbf{A}$ ;  $\mathbf{A}$  is connected to  $\mathbf{C}$  via:

$$A_{ik} = \left( \delta_{ik} \sum_{j=1}^N C_{jk} \right) - C_{ik}. \quad (1)$$

A whole series of works based on  $\mathbf{A}$  were devoted to classical deterministic and random graphs, such as Cayley-trees (dendrimers), hyperbranched macromolecules, the Erdős-Rényi (ER) random graph and bond diluted

Cayley-trees [17, 18, 19, 20, 21, 22, 23, 24, 25, 26, 27, 28, 29]. Based on the Laplacian, many time and frequency-dependent observables can be written as integrals over  $\rho(\lambda)$ , the density of eigenvalues of  $\mathbf{A}$ : The structure of these observables is either

$$Q(t) = \int_{0+}^{\infty} d\lambda f(t, \lambda) \rho(\lambda), \quad (2)$$

or some related form, in which  $t$  is replaced by  $\omega$ . For instance, for random walks, the site averaged return probability  $Q_R(t)$  of a random walker to the origin is obtained with the choice  $f_R(t, \lambda) = e^{-\lambda t}$  [22]. Moreover, the mechanical storage and loss moduli [26, 27], the averaged time-dependent stretching of macromolecules in external fields [26, 27], and the dielectric relaxation functions [30], all obey forms similar to Eq. (2). We are interested in the dynamic behavior of random graphs with arbitrary degree distributions and hence in the density  $\rho(\lambda)$  of their eigenfrequencies. Following the ideas used in the analysis of gel dynamics [20] and hyperbranched polymers [19], we display an integral equation for  $\rho(\lambda)$  for a special class of random graphs with arbitrary degree distributions [13, 31, 32, 33]. This integral equation allows us to determine  $\rho(\lambda)$  for the classes of scale-free networks discussed in Ref. [12].

## II. RANDOM GRAPHS WITH ARBITRARY DEGREE DISTRIBUTIONS

The ensemble of networks under consideration is obtained by starting from  $N$  vertices. Each vertex  $i$  has its degree  $k_i$ , and the probability distribution of the  $k_i$  is  $p_k$ . As discussed in Ref. [33], one can then connect the vertices pairwise through bonds (random pairing), while fulfilling the condition that the number of bonds emanating from each vertex  $i$  is given by its degree  $k_i$ . All such possible combinations create the ensemble. In the limit  $N \rightarrow \infty$  the probability that a certain vertex is involved in a closed loop of bonds vanishes like  $1/N$  [33]; thus, in this limit a typical network realization is a set of

connected treelike clusters. Such a treelike structure may also be created as follows: We start from a vertex, say  $i$ , whose random degree  $k$  is chosen from the given distribution  $p_k$ . Then each of the  $k_i$  bonds of vertex  $i$  ends in a new vertex. One must note now that the probability of reaching via a randomly chosen bond a vertex of degree  $k$  is proportional to  $kp_k$ , i.e. it obeys the distribution

$$q_k = \frac{kp_k}{\sum_{j=1}^{\infty} jp_j}. \quad (3)$$

It follows that we must now distribute the degrees of the newly produced vertices according to  $q_k$ , Eq. (3). The procedure is then continued step after step and stops only where no new bonds were produced in the previous step. The method creates all the random trees of the ensemble. Two examples of such ensembles are the bond diluted Cayley tree with functionality  $f$  [34], where  $p_k = \binom{f}{k} p^k (1-p)^{f-k}$ , and the Erdős-Rényi random graph, whose degree distribution is  $p_k = p^k e^{-p}/k!$  [33].

Depending on the  $p_k$ -distribution, the ensemble consists either exclusively of finite clusters or it includes an infinite, connected cluster, containing a finite fraction of the vertices of the system [35]. In Refs. [10, 33] it was shown that the condition for the existence of this infinite cluster (also called percolating cluster) is given by

$$\frac{\sum_{k=0}^{\infty} k(k-1)p_k}{\sum_{k=0}^{\infty} kp_k} > 1. \quad (4)$$

Eq. (4) defines the so-called percolation threshold. It is very useful to extend the present model, by also allowing the strength of each bond to be weighted [19, 20] following a normalized coupling strength distribution  $D(\mu)$ . Thus in the corresponding connectivity matrices, each of the nonzero values of  $C_{ik}$  can be chosen according to the distribution  $D(\mu)$ .

As mentioned above, for a given network cluster  $S$  various dynamical quantities involve only the density of eigenvalues  $\rho_S(\lambda)$  of the corresponding Laplacian  $\mathbf{A}^S$ . Now, the ensemble averaged density of eigenvalues is given by

$$\rho(\lambda) = \langle \rho_S(\lambda) \rangle \equiv \sum_S w_S \rho_S(\lambda), \quad (5)$$

where the sum extends over all the clusters  $S$ , each of the  $\rho_S(\lambda)$  is normalized, and  $w_S$  denotes the probability with which the cluster  $S$  is produced by the iterative growth procedure. Each of the  $S$  created in this way is connected, so that  $\mathbf{A}^S$  has only one zero eigenvalue, whose

corresponding eigenvector is homogeneous. It turns out to be convenient to split off from  $\rho(\lambda)$  the delta peak at  $\lambda = 0$  whose weight is  $\rho_0$ , by setting:

$$\rho(\lambda) = \rho_0 \delta(\lambda) + \rho_+(\lambda). \quad (6)$$

The density of states is connected with the diagonal elements of the resolvent, see e.g. Ref. [19]. Denoting for each site  $k$  the  $k$ -th diagonal element of the resolvent  $\mathbf{R}(\lambda) = (\mathbf{A}^S - \lambda \mathbf{1})^{-1}$  by  $R_{kk}(\lambda)$ , what is needed is  $R_{kk}(\lambda)$  averaged over all sites  $k$  and over all the  $S$ -clusters:

$$R(\lambda) = \langle (\mathbf{A}^S - \lambda \mathbf{1})_{kk}^{-1} \rangle. \quad (7)$$

The probability  $w_{k,S}$  that when creating  $S$  we start at site  $k$  does not depend on  $k$ ; one has thus  $w_{k,S} = w_S/|S|$ , where  $|S|$  denotes the number of vertices inside  $S$ . This leads to

$$\begin{aligned} R(\lambda) &= \sum_S \sum_{k=1}^{|S|} w_{k,S} (\mathbf{A}^S - \lambda \mathbf{1})_{kk}^{-1} \\ &= \sum_S w_S \frac{1}{|S|} \sum_{k=1}^{|S|} (\mathbf{A}^S - \lambda \mathbf{1})_{kk}^{-1}. \end{aligned} \quad (8)$$

Using for the normalized density of states of cluster  $S$  the relation

$$\rho_S(\lambda) = \lim_{\epsilon \rightarrow 0} \frac{1}{\pi} \frac{1}{|S|} \text{Im} \sum_{k=1}^{|S|} (\mathbf{A}^S - (\lambda + i\epsilon) \mathbf{1})_{kk}^{-1}, \quad (9)$$

we obtain from Eq. (5)

$$\rho(\lambda) = \lim_{\epsilon \rightarrow 0} \frac{1}{\pi} \text{Im} R(\lambda + i\epsilon), \quad (10)$$

with  $R(\lambda)$  being given by Eq. (7). Now, the average over the disorder can be performed with the help of the replica method [36].

### III. DERIVATION OF THE INTEGRAL EQUATION

In the following we denote the starting vertex by 0. To obtain the averaged trace of the resolvent we rewrite it with the help of a Gaussian integral over  $n$ -dimensional vectors  $\mathbf{r}_i$

$$R(\lambda) = \left\langle \left[ \text{Det} \frac{i(\mathbf{A}^S - \lambda \mathbf{1})}{2\pi} \right]^{n/2} \frac{i}{n} \int \left( \prod_j d\mathbf{r}_j \right) \mathbf{r}_0^2 \exp \left[ -\frac{i}{2} \left( \sum_{j,k} A_{jk}^S \mathbf{r}_j \mathbf{r}_k - \lambda \sum_j \mathbf{r}_j^2 \right) \right] \right\rangle, \quad (11)$$

see e.g. Ref. [19] for details. The averaging procedure in Eq. (11) is considerably simplified by taking the replica limit  $n \rightarrow 0$ , since then the  $n/2$ -th power of the determinant is unity. Using

$$\sum_{i < j} C_{ij}^S(\mathbf{r}_i - \mathbf{r}_j)^2 = \sum_{i,j} A_{ij}^S \mathbf{r}_i \mathbf{r}_j, \quad (12)$$

which follows readily from Eq. (1), leads to

$$R(\lambda) \doteq \frac{i}{n} \int \left( \prod_j d\mathbf{r}_j \right) \mathbf{r}_0^2 \exp \left[ i \frac{\lambda}{2} \sum_j \mathbf{r}_j^2 \right] \left\langle \exp \left[ -\frac{i}{2} \sum_{j < k} C_{jk}^S (\mathbf{r}_j - \mathbf{r}_k)^2 \right] \right\rangle \quad (13)$$

Here we use the dot over the equation sign to indicate that the limit  $n \rightarrow 0$  has to be taken. Now we employ the fact that the  $S$ -clusters are trees, in order to perform the integrations in Eq. (13) iteratively, following the number  $g$  of growth steps. After the first growth step we have

$$R^{(1)}(\lambda) \doteq \frac{i}{n} \int d\mathbf{r}_0 \mathbf{r}_0^2 \exp \left[ i \frac{\lambda}{2} \mathbf{r}_0^2 \right] \sum_{k=0}^{\infty} p_k \{ \phi^{(1)}(\mathbf{r}_0) \}^k, \quad (14)$$

where we defined

$$\phi^{(1)}(\mathbf{r}_0) \equiv \int d\mathbf{r} \exp \left[ i \frac{\lambda}{2} \mathbf{r}^2 \right] F(\mathbf{r}_0, \mathbf{r}) \quad (15)$$

and

$$F(\mathbf{r}_j, \mathbf{r}_k) = \int_0^{\infty} d\mu D(\mu) \exp \left[ -i \frac{\mu}{2} (\mathbf{r}_j - \mathbf{r}_k)^2 \right]. \quad (16)$$

In a similar way, the averaged diagonal element after the second growth step reads

$$R^{(2)}(\lambda) \doteq \frac{i}{n} \int d\mathbf{r}_0 \mathbf{r}_0^2 \exp \left[ i \frac{\lambda}{2} \mathbf{r}_0^2 \right] \sum_{k=0}^{\infty} p_k \{ \phi^{(2)}(\mathbf{r}_0) \}^k \quad (17)$$

with

$$\phi^{(2)}(\mathbf{r}_0) = \int d\mathbf{r} \exp \left[ i \frac{\lambda}{2} \mathbf{r}^2 \right] F(\mathbf{r}_0, \mathbf{r}) \sum_{k=1}^{\infty} q_k \{ \phi^{(1)}(\mathbf{r}) \}^{k-1}. \quad (18)$$

More generally, introducing the generating functions of the  $p_k$ 's and the  $q_k$ 's:

$$G_0(\phi) = \sum_{k=0}^{\infty} p_k \phi^k \quad \text{and} \quad G_1(\phi) = \sum_{k=1}^{\infty} q_k \phi^{k-1} = \frac{G_0'(\phi)}{G_0'(1)}, \quad (19)$$

we find that after  $g$  growth steps  $\phi^{(g)}(\mathbf{r})$  obeys:

$$\phi^{(g)}(\mathbf{r}_0) = \int d\mathbf{r} \exp \left[ i \frac{\lambda}{2} \mathbf{r}^2 \right] F(\mathbf{r}_0, \mathbf{r}) G_1[\phi^{(g-1)}(\mathbf{r})], \quad (20)$$

and that it can be obtained iteratively, starting from  $\phi^{(1)}(\mathbf{r})$  given by Eq. (15). Furthermore,  $R^{(g)}(\lambda)$  fulfills

$$R^{(g)}(\lambda) \doteq \frac{i}{n} \int d\mathbf{r}_0 \mathbf{r}_0^2 \exp \left[ i \frac{\lambda}{2} \mathbf{r}_0^2 \right] G_0[\phi^{(g)}(\mathbf{r}_0)]. \quad (21)$$

Now, the  $n \rightarrow 0$  limit can be performed as described in Ref. [19]. This leads for  $g \rightarrow \infty$  to the pair of equations

$$R(\lambda) = -\frac{1}{\lambda} \int_0^{\infty} dx e^{-x} G_0[\phi(x)] \quad (22)$$

and

$$\phi(x) = \hat{\mathbf{O}} e^{-x} G_1[\phi(x)], \quad (23)$$

where  $\hat{\mathbf{O}}$  is the linear operator

$$\begin{aligned} \hat{\mathbf{O}} &= \int_0^{\infty} d\mu D(\mu) \exp \left[ -\frac{\lambda}{\mu} x \partial_x^2 \right] \\ &= \sum_{k=0}^{\infty} \frac{\langle \mu^{-k} \rangle_{\mu}}{k!} (-\lambda)^k (x \partial_x^2)^k, \end{aligned} \quad (24)$$

where  $\langle \dots \rangle_{\mu}$  denotes the average over the distribution  $D(\mu)$ .

In Ref. [33] it was shown that the generating function  $H_0(z) = \sum_{s=1}^{\infty} P_s z^s$  of the probabilities  $P_s$  that a randomly chosen vertex is part of a cluster of  $s$  vertices can be obtained based on the relations

$$H_0(z) = z G_0(H_1(z)) \quad \text{and} \quad H_1(z) = z G_1(H_1(z)). \quad (25)$$

Here  $H_1(z)$  is the generating function for the distribution of sizes of components that are reached by choosing a random bond and following it to one of its ends. As a check for our scheme we now show that our Eqs. (22) and (23) are consistent with Eqs. (25). To do this we look for a solution of Eq. (23) in the form of a power series in  $\lambda$

$$\phi(x) = \sum_{k=0}^{\infty} \lambda^k \phi_k(x). \quad (26)$$

We obtain the first term by comparing powers of  $\lambda$ :

$$\phi_0(x) = e^{-x} G_1(\phi_0(x)). \quad (27)$$

Identifying  $e^{-x}$  with  $z$ , Eq. (27) reproduces the second Eq. (25) with  $\phi_0(x) = H_1(e^{-x})$ . Hence we infer from the first Eq. (25) that

$$e^{-x} G_0(\phi_0(x)) = \sum_{s=1}^{\infty} P_s e^{-sx}. \quad (28)$$

It follows that  $G_0[\phi_0(0)]$  is the probability for a vertex to be part of a finite size cluster.

From Eqs. (6) and (10) one infers that  $R(\lambda)$  possesses a simple pole of the form  $\rho_0/\lambda$ , where  $\rho_0$  is the finite weight of zero eigenvalues. Now  $\rho_0$  can be calculated by inserting Eq. (26) into Eq. (22), which leads to

$$\begin{aligned}\rho_0 &= \int_0^\infty dx e^{-x} G_0(\phi_0(x)) \\ &= 1 + G'_0(1) \int_0^\infty dx e^{-x} G_1(\phi_0(x)) \phi'_0(x) \quad (29) \\ &= 1 + G'_0(1) \int_0^\infty dx \phi_0(x) \phi'_0(x) = 1 - \frac{G''_0(1)}{2}, \quad (30)\end{aligned}$$

where in the second step we performed a partial integration and used Eq. (19). We note that inserting Eq. (28) into (30) leads to  $\rho_0 = \sum_{s=1}^\infty P_s/s$ ; the result represents the fact that each  $s$ -cluster contributes a term  $1/s$  to the density of the eigenvalue zero.

#### IV. SCALE-FREE NETWORKS CLOSE TO THEIR PERCOLATION THRESHOLD

In this section we turn from our general considerations to focus on *scale-free* degree distributions; these exhibit for  $k$  large a power-law behavior,  $p_k \sim k^{-\gamma}$ . To describe the distance from the percolation threshold, Eq. (4), we introduce the parameter  $\Delta$  through the relation

$$\Delta = 1 - \frac{\sum_{k=0}^\infty k(k-1)p_k}{\sum_{k=0}^\infty k p_k} = 1 - G'_1(1). \quad (31)$$

Evidently, we assume by this that the first and the second moments of the  $p_k$  distribution exist. From Eq. (4) it follows that for  $\Delta > 0$  the ensemble is made up of finite connected clusters, while for  $\Delta < 0$  there exists an infinite cluster. The critical point (percolation threshold) is at  $\Delta = 0$ . As a note of caution we remark that the choice of the sign of  $\Delta$  is possibly misleading but since in the following we investigate exclusively network clusters below the percolation threshold this choice considerably simplifies the formulas. Exemplarily, for the ER random graph the critical point is at  $p_c = 1$  and for the bond diluted Cayley tree it is at  $p_c = 1/(f-1)$ ; using Eq. (31) it turns out that in both cases  $\Delta = (p_c - p)/p_c$ . Note that for  $\gamma < 3$  Eq. (31) diverges; this agrees with the criterium of Eq. (4), since for  $\gamma < 3$  one always has an infinite cluster [10].

We center now on the form of Eqs. (23) and (22) close to  $\Delta = 0$ . To be sufficiently general, we assume  $p_k$  to have for large  $k$  the form

$$p_k \sim k^{-\gamma} \{c + O(k^{-1})\}. \quad (32)$$

This implies for  $\gamma > 3$  that the power series of  $G_1(\phi)$ , Eq. (19), has as radius of convergence the unit circle  $|\phi| = 1$ . To determine the singularity on the radius of convergence we remark that the expansion coefficients

$\tilde{p}_k$  of the quantity  $\tilde{G}_1(\phi) \equiv G_1(\phi) - c\Gamma(2-\gamma)(1-\phi)^{\gamma-2}$  obey  $\tilde{p}_k \sim k^{-\gamma-1}$  for large  $k$ . Thus  $\tilde{G}_1(\phi)$  is  $m$ -times continuously differentiable for  $|\phi| \leq 1$ , where  $m$  is the largest integer smaller than  $\gamma - 2$ . Using the Taylor expansion of  $\tilde{G}_1(\phi)$  around  $\phi = 1$  up to order  $m$  one gets [12, 37]

$$\begin{aligned}G_1(\phi) &\simeq 1 + (1-\Delta)(\phi-1) + \dots \quad (33) \\ &\quad + \frac{1}{m!} \partial_\phi^m G_1(1) (\phi-1)^m + c\Gamma(2-\gamma)(1-\phi)^{\gamma-2},\end{aligned}$$

where we used Eq. (31). Close to the percolation threshold  $\Delta = 0$  we expect the solution of Eq. (23) to scale in its variables  $x$  and  $\lambda$ , and we choose a solution of the form [21]

$$\phi(x) \simeq 1 - \Delta^\beta \tilde{\phi}(x/\Delta^\delta, \lambda/\Delta^{1+\delta}), \quad (34)$$

with exponents  $\beta > 0$  and  $\delta > 0$ , to be determined below. Inserting Eq. (34) into Eq. (23) and expanding in powers of  $\Delta$  by using Eq. (34) we obtain

$$\begin{aligned}1 - \Delta^\beta \tilde{\phi}(x, \lambda) &= \quad (35) \\ &\left\{ 1 - \langle \mu^{-1} \rangle \lambda \Delta x \partial_x^2 + \dots \right\} \left\{ 1 - \Delta^\delta x + \dots \right\} \times \\ &\left\{ 1 - (1-\Delta) \Delta^\beta \tilde{\phi}(x, \lambda) + \theta(\gamma-4) \frac{G''_1(1)}{2} \Delta^{2\beta} \tilde{\phi}^2(x, \lambda) \right. \\ &\quad \left. + \theta(4-\gamma) c\Gamma(2-\gamma) \Delta^{\beta(\gamma-2)} \tilde{\phi}^{\gamma-2}(x, \lambda) + \dots \right\},\end{aligned}$$

where  $\theta(x)$  denotes the Heaviside function and the dots indicate terms with higher powers of  $\Delta$ . Comparing powers of  $\Delta$  leads to the equation

$$\begin{aligned}0 &= \langle \mu^{-1} \rangle \lambda \Delta^{1+\beta} x \partial_x^2 \tilde{\phi}(x) - \Delta^\delta x + \Delta^{\beta+1} \tilde{\phi}(x) \\ &\quad + \theta(\gamma-4) \frac{G''_1(1)}{2} \Delta^{2\beta} \tilde{\phi}^2(x) \\ &\quad + \theta(4-\gamma) c\Gamma(2-\gamma) \Delta^{\beta(\gamma-2)} \tilde{\phi}^{\gamma-2}(x).\end{aligned} \quad (36)$$

Now the unknown exponents  $\beta$  and  $\delta$  are determined by the requirement that all terms in this equation be of the same order in  $\Delta$ . For  $\gamma > 4$  this leads to  $\beta = 1$  and  $\delta = 2$ . From Eq. (36) it follows then:

$$0 = \langle \mu^{-1} \rangle \lambda x \partial_x^2 \tilde{\phi}(x) - x + \tilde{\phi}(x) + \frac{G''_1(1)}{2} \tilde{\phi}^2(x), \quad (37)$$

This universal scaling equation for the order parameter field  $\tilde{\phi}(x)$  was already pointed out in Ref. [21] in connection with the mean-field theory of random resistor networks. Thus for  $\gamma > 4$  we obtain the classical mean-field scaling equation of the order parameter field  $\phi(x)$ , which is also valid for the ER graph and the Cayley-tree. This is in accordance with the result in Ref. [12], that the critical properties of classical random graphs are *not* changed for  $\gamma > 4$ . On the other hand, for  $3 < \gamma < 4$  the exponents  $\beta$  and  $\delta$  read now  $\delta = 1 + \beta$  and  $\delta = \beta(\gamma - 2)$ , so that, solving for  $\beta$ :

$$\beta = \frac{1}{\gamma - 3}, \quad (38)$$

as found in Refs. [11] and [12]. Now the corresponding equation reads

$$0 = \langle \mu^{-1} \rangle \lambda x \partial_x^2 \tilde{\phi}(x) - x + \tilde{\phi}(x) + c\Gamma(2-\gamma)\tilde{\phi}^{\gamma-2}(x). \quad (39)$$

We note that  $\beta$  is related to the probability  $P_\infty \sim \Delta^\beta$  that a vertex belongs to the percolating cluster. From Eqs. (37) and (39) for the order parameter field  $\tilde{\phi}$  we obtain a scaling relation for  $R(\lambda)$  by inserting Eq. (34) into Eq. (22). To this end we subtract the pole  $\rho_0/\lambda$  from  $R(\lambda)$  and expand in powers of  $\Delta$ :

$$\begin{aligned} R(\lambda) - \frac{\rho_0}{\lambda} &= -\frac{1}{\lambda} \int_0^\infty dx e^{-x} \{G_0(\phi(x)) - G_0(\phi_0(x))\} \\ &\simeq -\frac{\Delta^{1+\beta}}{\lambda} \int_0^\infty dx e^{-\Delta^{1+\beta}x} \\ &\quad \times \{G_0(1 - \Delta^\beta \tilde{\phi}(x, \lambda/\Delta^{2+\beta})) - G_0(1 - \Delta^\beta \tilde{\phi}_0(x))\} \\ &\simeq \Delta^{\beta-1} \frac{\langle k \rangle}{\lambda/\Delta^{2+\beta}} \int_0^\infty dx \left\{ \tilde{\phi}(x, \lambda/\Delta^{2+\beta}) - \tilde{\phi}_0(x) \right\} \end{aligned} \quad (40)$$

where  $\tilde{\phi}_0(x) = \lim_{\Delta \rightarrow 0} \Delta^{-\beta} \{ \phi_0(x \Delta^{1+\beta}) - 1 \}$ . Thus we have shown that  $\rho_+(\lambda)$  obeys for  $\lambda \sim \Delta$  close to 0 a scaling law of the form

$$\rho_+(\lambda, \Delta) \simeq \Delta^{\beta-1} \tilde{\rho}(\lambda/\Delta^{2+\beta}). \quad (41)$$

Furthermore, the scaling function  $\tilde{\rho}(x)$  can be determined via Eqs. (40), (37), (39), and (10). From the preceding considerations it follows immediately that the shape of  $\tilde{\rho}(\lambda)$  differs in the region  $\gamma > 4$  from its shape in the region  $3 < \gamma < 4$ . In the first region Eq. (37) is valid and  $\tilde{\rho}(\lambda)$  does not depend on  $\gamma$ , whereas in the second region the  $\gamma$ -dependent Eq. (39) holds.

## V. INTEGRATION FOR SCALE FREE DEGREE DISTRIBUTIONS AND SPECIAL DISTRIBUTIONS OF BOND STRENGTHS

As shown in Ref. [20], the analytical work simplifies considerably for the following distribution of bond strengths:

$$D(\mu) = \frac{1}{\mu^2} \exp(-1/\mu), \quad (42)$$

since then the operator  $\hat{\mathbf{O}}$ , Eq. (24), takes the form

$$\hat{\mathbf{O}} = \int_0^\infty d\mu \frac{1}{\mu^2} \exp(-1/\mu) \exp\left[-\frac{\lambda}{\mu} x \partial_x^2\right] = [1 + \lambda x \partial_x^2]^{-1} \quad (43)$$

For instance, applying  $1 + \lambda x \partial_x^2 = \hat{\mathbf{O}}^{-1}$  to both sides of Eq. (23), one obtains the ordinary second order differential equation

$$\phi(x) + \lambda x \partial_x^2 \phi(x) = e^{-x} G_1[\phi(x)]. \quad (44)$$

As noted in Ref. [20], the particular choice of  $D(\mu)$ , Eq. (42), does not change much the small  $\lambda$  behavior of  $\rho(\lambda)$ , given that in Eq. (42) the probability for small coupling strengths  $\mu$  is exponentially small. In particular,  $D(\mu)$  does not change the form of the function  $\tilde{\rho}(\lambda)$ , as only the first inverse moment  $\langle \mu^{-1} \rangle$  enters Eqs. (37) and (39). Eq. (44) has to be solved subject to the boundary conditions

$$\phi(0) = 1 \quad \text{and} \quad \phi(\infty) = 0. \quad (45)$$

In the limit  $\lambda \rightarrow 0$  Eq. (44) can be linearized around the first term  $\phi_0(x)$  of the asymptotic expansion, Eq. (26). This is achieved by inserting  $\phi(x) = \phi_0(x) + \phi_l(x)$  into Eq. (44) and keeping only linear terms in  $\phi_l$ , since from Eq. (26) we have  $\phi_l(x) = O(\lambda)$ . This results in the inhomogeneous linear equation

$$\lambda x \partial_x^2 \phi_l(x) + \{1 - e^{-x} G_1'[\phi_0(x)]\} \phi_l(x) = -\lambda x \partial_x^2 \phi_0(x). \quad (46)$$

To investigate specific scale-free degree distributions we choose the following generating function

$$\begin{aligned} G_0(\phi) &= \phi + \frac{1}{2}(1-\Delta)(1-\phi)^2 - \frac{1}{9} \frac{\gamma-3}{\gamma-4} (1-\phi)^3 \\ &\quad + \frac{2}{3} \frac{1}{(\gamma-4)(\gamma-2)(\gamma-1)} (1-\phi)^{\gamma-1}. \end{aligned} \quad (47)$$

This form corresponds indeed to a degree distribution  $p_k$  which obeys Eq. (32); the  $c$ -value in Eq. (32) is

$$c = \frac{2}{3} \frac{1}{(\gamma-4)(\gamma-2)(\gamma-1)\Gamma(1-\gamma)}. \quad (48)$$

The algebraic choice of  $G_0(\phi)$  given by Eq. (47) reduces considerably the effort needed to integrate Eq. (44). Furthermore, Eq. (47) can be used in the whole interval  $3 < \gamma < 5$  containing the value  $\gamma = 4$  above which regular mean-field exponents of percolation appear. On the other hand, for values of  $\gamma$  outside the interval  $3 < \gamma < 5$  not all expansion coefficients of  $G_0(\phi)$  are non-negative and thus they cannot be viewed anymore as probabilities. Note that the poles in  $4 - \gamma$  of the last two terms in Eq. (47) cancel and expanding Eq. (47) in powers of  $4 - \gamma$  we obtain for  $\gamma = 4$  a branching point of the form  $(1 - \phi)^3 \log(1 - \phi)$  at  $\phi = 1$ . Furthermore, from Eq. (30) it follows that  $G_0(\phi)$  of Eq. (47) leads to  $\rho_+(\lambda)$  being normalized to:

$$\int_0^\infty d\lambda \rho_+(\lambda) = \frac{1}{2}. \quad (49)$$

### A. Numerical procedure

To numerically calculate the eigenvalue spectra of scale-free networks we have performed extensive numerical diagonalizations of the Laplacians of these structures.

We create our structures by the recursive scheme introduced in the second section: For each realization of

the structure we first begin with an initial vertex, whose functionality  $k$  is determined according to the probabilities  $p_k$  derived from the generating function Eq. (47). At the open end of each bond a new  $k'$ -functional vertex is placed, now with  $k'$  distributed according to the probability distribution  $q_{k'}$  given in Eq. (3); the latter procedure is then applied recursively to the  $k' - 1$  open bonds of this new vertex. The recursion stops when no open bonds are left, i.e. when all outer vertices have functionality  $k' = 1$ . Note, however, that due to the limited time and memory resources available for the subsequent diagonalizations, the total number of bonds has to be restricted to some maximum value  $N_{\max}$ . If a given recursion has not stopped before reaching a total of  $N_{\max}$  bonds we proceed by closing all remaining open ends by a  $k' = 1$ -vertex and evaluate the properties of this truncated structure. Obviously, this also limits the range of validity of the resulting spectrum. As observed in our previous study [19], in the region affected by the truncation the spectrum shows characteristic oscillations. To verify this procedure for the truncation limit  $N_{\max} = 500$  used in general in this study, we have also performed for some of the curves shown in Fig.4 additional diagonalizations using  $N_{\max} = 4000$ . The so obtained numerical results for  $\log_{10} \rho(\lambda)$  agree within the symbol size for the whole range covered by the  $N_{\max} = 500$  data shown in Fig.4 and in fact extend the range of agreement with the solution of the differential Eq. (44) by one order of magnitude.

For the distribution of bond strength of a given structure we chose either fixed bond strengths  $\mu = 1$  or strengths  $\mu$  distributed according to Eq. (42). The connectivity matrix  $\mathbf{A}_{ij}$  with entries weighted by these  $\mu$  is, by construction, a real, symmetric matrix. For all these matrices we obtained the eigenvalues using a combination of the Householder method and of the tridiagonal QL diagonalization algorithm [38, 39].

We accumulated the eigenvalues of all structures generated for specific values of the parameters  $\gamma$  and  $\Delta$ , where eigenvalues stemming from a structure with  $|S|$  monomers are weighted with a factor of  $1/|S|$ , as given by Eqs. (5) and (9). For each of the data sets shown later in Figs 1, 3, and 4 the total number of structures truncated at  $N_{\max} = 500$  was  $5 \cdot 10^7$  and for structures truncated at  $N_{\max} = 4000$  was  $4 \cdot 10^5$ .

## VI. RESULTS

In Fig. 1 we display first the density of eigenvalues  $\rho(\lambda)$  for the degree distribution  $p_k$  generated by  $G_0(\phi)$ , Eq. (47), with  $\gamma = 3.5$  and for various values of  $\Delta \leq 0$ . The random coupling strengths  $\mu$  obey the distribution of Eq. (42). We obtained  $\rho(\lambda)$  both through the numerical integration of Eq. (44) and also through the direct numerical diagonalization of many structure realizations, as described above. As can be seen, the  $\rho(\lambda)$  obtained by the two methods agree very well with each other over

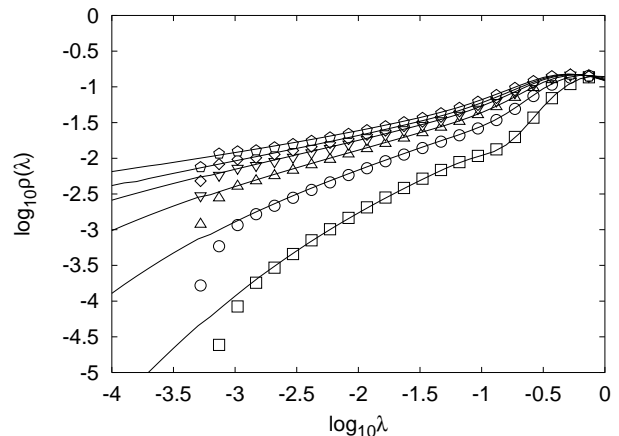


FIG. 1: Density of eigenvalues  $\rho(\lambda)$  in double logarithmic scales. Displayed are spectra for the scale free degree distribution generated by  $G_0(\phi)$ , Eq. (47), and random coupling strengths  $\mu$  obeying Eq. (42). Here,  $\gamma = 3.5$  is fixed and  $\Delta$  is  $0(\diamond)$ ,  $0.02(\diamond)$ ,  $0.04(\nabla)$ ,  $0.08(\triangle)$ ,  $0.16(\circ)$ , and  $0.32(\square)$  from above. Lines: numerical solution of Eq. (44). Symbols: direct diagonalization of randomly created structures.

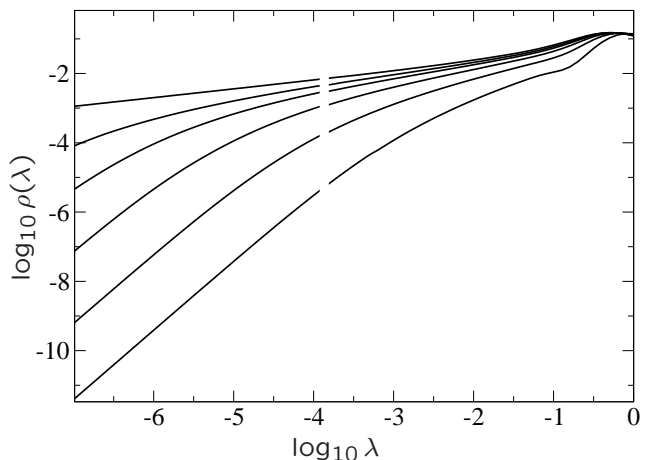


FIG. 2: Density of eigenvalues  $\rho(\lambda)$ , obtained from the integration of Eq. (44) (right hand side of the figure) and from Eq. (46) (left hand side) for the same parameter values as in Fig. 1. To render this difference clear, we have left out a small region around  $\log_{10} \lambda = -3.8$ .

a large  $\lambda$ -range, thus supporting our theoretical considerations. The deviations of the curves from each other for small  $\lambda$  are due to the limitations imposed by our direct diagonalization approach; in fact the sharp decay of the numerical results for  $\lambda < 10^{-3}$  is an artefact. The curves of Fig. 1 possess a shoulder at  $\log_{10} \lambda \simeq -0.7$  which is most evident for the lowest curve corresponding to  $\Delta = 0.32$ . However, this structure is caused by the choice  $G_0(\phi)$ , Eq. (47), and is not specific for scale-free degree distributions. As discussed above, scale-free networks are characterized by the behavior for *small values* of  $\lambda$ . To investigate the small  $\lambda$  behavior, we show in Fig.

2  $\rho(\lambda)$  for the same values of the parameters  $\gamma$  and  $\Delta$ , but extending to much smaller values of  $\lambda$ . In this plot the results below  $\lambda < 10^{-3.8}$  are obtained from the linearized Eq. (46), an approximation which we expect to be exact in the limit  $\lambda \rightarrow 0$ . In fact, at  $\lambda = 10^{-3.8}$ , where the approximation and the exact curve get together, the relative error of  $\rho(\lambda)$  amounts to about 1%, which is already hard to observe in the plots. For  $\Delta$  not too close to the percolation threshold at  $\Delta = 0$  and for small  $\lambda$  the slopes of the curves in the double logarithmic plot of Fig. 2 tend to a constant. This would imply a simple algebraic dependence:

$$\rho(\lambda) \sim c(\Delta)\lambda^{\alpha_1}, \text{ for } \lambda \rightarrow 0, \quad (50)$$

with a positive exponent  $\alpha_1$  and a  $\Delta$ -dependent coefficient  $c(\Delta)$ . This differs from the situation expected to hold on classical random graphs with sufficiently fast decaying degree distributions  $p_k$ , where heuristic arguments have been given [20, 22] for the existence of Lifshitz tails in the density of states. In the latter situation one should observe the form [19]

$$\rho(\lambda) \sim \exp\left[-\frac{A(\Delta)}{\sqrt{\lambda}}\right], \text{ for } \lambda \rightarrow 0, \quad (51)$$

where  $A(\Delta) \sim \Delta^{3/2}$  for  $\Delta \rightarrow 0$ . This behavior stems from the fact that small eigenvalues are produced by large, quasi linear regions, which however, occur with very small probability. Since for scale free degree distributions such linear regions are not likely to occur, there have to be other types of configurations which lead to an increase in the occurrence of small eigenvalues. For instance two vertices, each of very large degree, moving against each other produce a very low eigenvalue.

At the percolation threshold  $\Delta = 0$  we infer from Fig. 2 for small  $\lambda$  an algebraic decay of the form of Eq. (50), with an exponent  $\alpha_2$ , which however differs from  $\alpha_1$ . One has namely  $\alpha_2 < \alpha_1$ . Thus close to  $\Delta = 0$  we encounter here a crossover behavior between two algebraic decays with different powers  $\alpha_1$  and  $\alpha_2$ . The scaling Eq. (41) suggests that this crossover should take place at  $\lambda \sim \Delta^{2+\beta}$ .

To determine the  $\gamma$  dependence of  $\alpha_2$ , we display in Fig. 3  $\rho(\lambda)$  in double logarithmic scales for  $\Delta = 0$  and for various values of  $\gamma$ . Assuming that for  $\lambda \rightarrow 0$  the slopes of the plotted curves tend to a constant, say  $\alpha_2$  we infer for  $\gamma = 4.5, 4.25, 4, 3.75, 3.5$  and  $3.25$  the values  $\alpha_2 = 0.017, 0.015, 0.04, 0.113, 0.25$  and  $0.5$ , respectively. For  $\gamma > 4$  we expect to encounter the classical mean-field scaling function; since then  $\rho(\lambda)$  tends to a constant for  $\lambda \rightarrow 0$  at  $\Delta = 0$  [19, 20], this implies that  $\alpha_2 = 0$  which is in good agreement with the first two values  $\alpha_2 = 0.017$  for  $\gamma = 4.5$  and  $\alpha_2 = 0.015$  for  $\gamma = 4.25$ . Moreover, directly at  $\gamma = 4$ , we expect possible logarithmic corrections to the power law, Eq. (50) which explains the value  $\alpha_2 = 0.04$  which is slightly too large. For  $3 < \gamma < 4$  it turns out that we can reproduce the  $\gamma$ -dependence of  $\alpha_2$  through

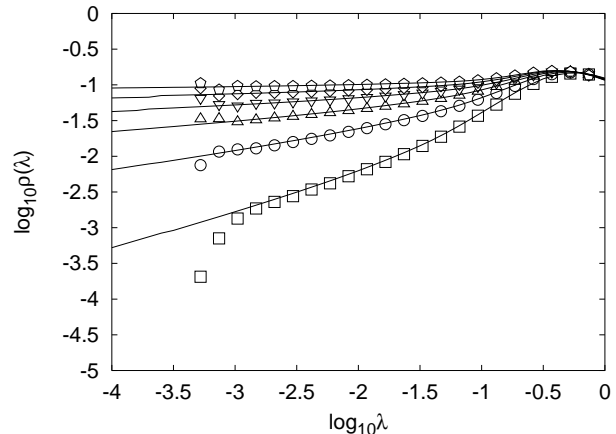


FIG. 3: Density of eigenvalues  $\rho(\lambda)$  in double logarithmic scales at the percolation threshold  $\Delta = 0$  for  $G_0(\phi)$ , Eq. (47) and  $\mu$  obeying Eq. (42). Here  $\gamma$  is varied, being taken to be  $\gamma = 4.5(\circ), 4.25(\diamond), 4(\nabla), 3.75(\triangle), 3.5(\circ)$  and  $3.25(\square)$  from above. Lines: integration of Eq. (44), Symbols: direct diagonalization.

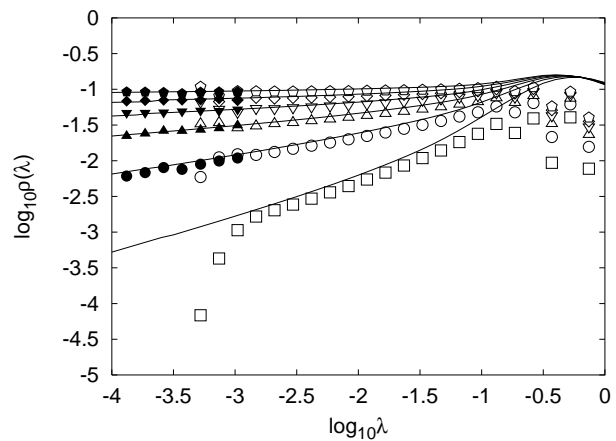


FIG. 4: Density of eigenvalues  $\rho(\lambda)$  at the percolation threshold  $\Delta = 0$  for fixed coupling strengths,  $\mu = 1$  in comparison with the analytical results for  $\mu$  obeying Eq. (42) (straight lines). The symbols show simulation data truncated at  $N_{\max} = 500$  (open symbols) and  $N_{\max} = 4000$  (filled symbols). The values of  $\gamma$  and  $\Delta$  and the symbol shapes are as in Fig.3

the relation:

$$\alpha_2 = \frac{4 - \gamma}{2\gamma - 5}. \quad (52)$$

In a similar way, we obtain from the small  $\lambda$  behavior of  $\rho(\lambda)$  for  $\Delta > 0$  that  $\alpha_1 = 2\gamma - 5$  holds.

The  $\gamma$  dependence of  $\alpha_2$  can be derived from the scaling relation Eq. (41) by using the fact that the behavior of  $\tilde{\rho}(\lambda)$  for  $\lambda \gg 1$  is given by the algebraic dependence of

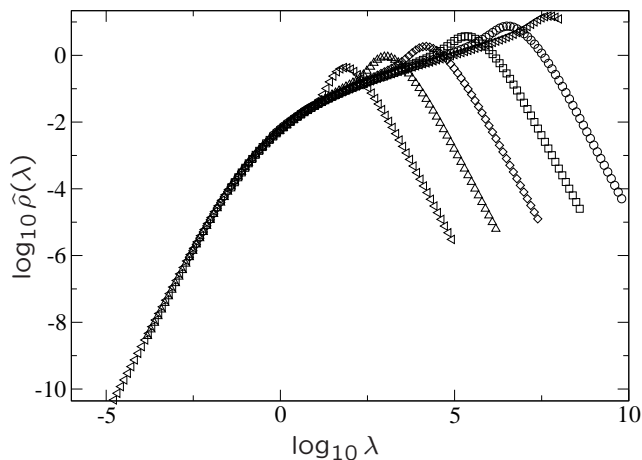


FIG. 5: The quantity  $\hat{\rho}(\lambda, \Delta) = \Delta^{-1}\rho(\lambda\Delta^4)$ , for  $\gamma = 3.5$  in double logarithmic scales. The different curves correspond to  $\Delta = 0.01, 0.02, 0.04, 0.08$  and  $0.16$  from the right.

$\rho(\lambda)$  for  $\lambda \ll 1$  at  $\Delta = 0$

$$\begin{aligned} \tilde{\rho}(\lambda) &= \lim_{\Delta \rightarrow 0} \Delta^{1-\beta} \rho(\lambda\Delta^{2+\beta}, \Delta) \sim \Delta^{1-\beta} (\lambda\Delta^{2+\beta})^{\alpha_2} \\ &= \Delta^{1-\beta+\alpha_2(2+\beta)} \lambda^{\alpha_2}. \end{aligned} \quad (53)$$

For this to give a reasonable limit the exponent  $1 - \beta + \alpha_2(2+\beta) = 0$  of  $\Delta$  has to vanish and solving this equation for  $\alpha_2$  proves the relation Eq. (52). Similarly, the behavior of  $\tilde{\rho}(\lambda)$  for  $\lambda \ll 1$  can be derived from the algebraic dependence Eq. (50) of  $\rho(\lambda)$  for  $\lambda \ll 1$  and  $\Delta > 0$

$$\begin{aligned} \tilde{\rho}(\lambda) &= \lim_{\Delta \rightarrow 0} \Delta^{1-\beta} \rho(\lambda\Delta^{2+\beta}, \Delta) \sim \Delta^{1-\beta} c(\Delta) (\lambda\Delta^{2+\beta})^{\alpha_1} \\ &= \Delta^{1-\beta+\alpha_1(2+\beta)} c(\Delta) \lambda^{\alpha_1}. \end{aligned} \quad (54)$$

By the same arguments as above this leads to  $c(\Delta) \sim \Delta^{\beta-1-\alpha_1(2+\beta)}$ , but does not fix the exponent  $\alpha_1$ .

As shown by Eqs. (39) and (40), the scaling function  $\tilde{\rho}(\lambda)$  of Eq. (41) should be model independent and therefore should not depend on the particular choice of  $D(\mu)$ , Eq. (42). In particular, at  $\Delta = 0$  a power law with the exponent  $\alpha_2$  should still hold. This is corroborated by Fig. 4, in which we display the density of eigenvalues  $\rho(\lambda)$  for fixed bond strengths,  $\mu = 1$ , obtained from the direct diagonalization of random matrices, together with the analytical results for the distribution, Eq. (42), of coupling strengths.

To investigate the range of validity of the scaling law Eq. (41) we display in double logarithmic scales for fixed  $\gamma = 3.5$  in Fig. 5 and  $\gamma = 4.5$  in Fig. 6 the quantity  $\hat{\rho}(\lambda, \Delta) \equiv \Delta^{1-\beta} \rho(\lambda\Delta^{2+\beta}, \Delta)$  which tends for  $\Delta \rightarrow 0$  to the scaling function  $\tilde{\rho}(\lambda)$  of Eq. (41). In both figures we show curves for various values of  $\Delta$  close to  $\Delta = 0$ . For  $\lambda$  and  $\Delta$  small enough the curves for  $\hat{\rho}(\lambda, \Delta)$  should collapse into a single one, given by the scaling function  $\tilde{\rho}(\lambda)$  of Eq. (41). In Fig. 5 the collapse appears roughly for  $\lambda\Delta^4 < 10^{-2}$  and in Fig. 6 for  $\lambda\Delta^3 < 10^{-2}$ . In Figs. 5 and 6 the scaling functions  $\tilde{\rho}(\lambda)$  are given by

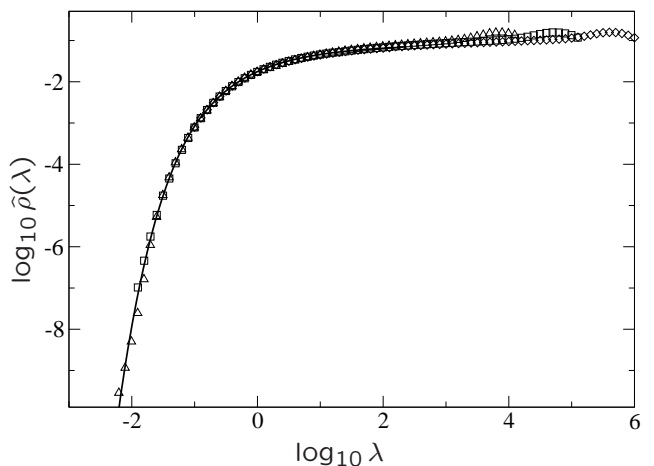


FIG. 6: The quantity  $\hat{\rho}(\lambda, \Delta) = \rho(\lambda\Delta^3)$  for  $\gamma = 4.5$  in double logarithmic scales. We show curves for  $\Delta = 0.01$  (diamonds),  $\Delta = 0.02$  (squares) and  $\Delta = 0.04$  (triangles). In addition, we display as a solid line the exact scaling function obtained by solving Eq. (37).

the envelopes of the curves  $\hat{\rho}(\lambda, \Delta)$  for different values of  $\Delta$ . These envelopes  $\tilde{\rho}(\lambda)$  seem to be monotonic growing functions. In Fig. 5  $\tilde{\rho}(\lambda)$  shows for the limiting case  $\lambda \rightarrow 0$  the algebraic behavior  $\tilde{\rho}(\lambda) \sim \lambda^{\alpha_1}$  but in Fig. 6 it is not possible to observe any algebraic dependence.

In Fig. 6, the function  $\tilde{\rho}(\lambda)$  given as a solid line is obtained from the direct integration of Eq. (37), which scales. More generally, for  $\gamma > 4$  we obtain  $\beta = 1$ ; we note that for  $\gamma > 4$  all network ensembles lead to the same scaling function  $\tilde{\rho}(\lambda)$ . Note that the derivation of Eqs. (37) and (40) in Sec. IV shows that the essential condition for this scaling function to hold is that the degree distribution  $p_k$  decay faster than  $k^{-4}$ . This condition is certainly fulfilled for classical random graphs, like the bond diluted Cayley tree or the Erdős-Rényi random graph.

## VII. CONCLUSIONS

In this work we investigated the eigenvalues of Laplacians of structures belonging to a general type of tree-like networks, in which the vertex degrees are randomly distributed. The Laplacian is of special interest, since it determines several, very important dynamic quantities associated with the network. For degree distributions  $p_k$  with a power law tail,  $p_k \sim k^{-\gamma}$ , we obtained  $\rho(\lambda)$ , the ensemble averaged density of eigenvalues, based on two different methods. First, in a traditional way, by performing numerical diagonalization techniques [14, 15]; second, using the replica method of statistical physics. The second approach allows to evaluate the ensemble averaged  $\rho(\lambda)$  based on an analytical integral equation. For large  $\lambda$ -domains it turns out that the agreement between the results obtained by the two methods is very good.



Of special interest is the behavior of  $\rho(\lambda)$  close to the percolation threshold. Here an infinite cluster appears, and it is known that the exponent  $\gamma$  which governs the large  $k$  behavior of  $p_k$  affects the critical exponents of the percolation problem [12]. With the help of our integral equation approach we were able to study the scaling properties of  $\rho(\lambda)$  close to the percolation threshold and to determine numerically the corresponding,  $\gamma$ -dependent scaling functions. In agreement with Ref. [12], we find that in the region  $\gamma > 4$  one recovers the critical properties of classical random graphs.

The long time dynamics is governed by the small  $\lambda$  behavior of  $\rho(\lambda)$ . For this we found two algebraic forms  $\rho(\lambda) \sim \lambda^{\alpha_1}$  and  $\rho(\lambda) \sim \lambda^{\alpha_2}$ , where the first relation holds *below* and the second *at* the percolation threshold. On the

basis of the numerical results of the integral equation we conjecture that  $\alpha_1 = 2\gamma - 5$  and  $\alpha_2 = (4 - \gamma)/\alpha_1$  hold. We find that in scale-free networks very small eigenvalues occur with higher probability than in classical random graphs. We conjecture that this finding is due to the existence of highly connected vertices.

### Acknowledgments

The support of the DFG, of the Fonds der Chemischen Industrie and of the BMBF are gratefully acknowledged. We are much indebted to Profs. S. Havlin and Y. Holovatch for enlightening discussions.

- 
- [1] A. L. Barabási and R. Albert, *Science* **286**, 509 (1999).  
 [2] A. L. Barabási, H. Jeong, and R. Albert, *Nature* **401**, 130 (1999).  
 [3] P. Erdős and A. Rényi, *The art of counting* (MIT Press, Cambridge, 1973).  
 [4] D. J. Watts and S. H. Strogatz, *Nature (London)* **393**, 440 (1998).  
 [5] M. E. J. Newman and D. J. Watts, *Phys. Rev. E* **60**, 7332 (1999).  
 [6] S. Jespersen, I. M. Sokolov, and A. Blumen, *J. Chem. Phys.* **113**, 7652 (2000).  
 [7] S. Jespersen and A. Blumen, *Phys. Rev. E* **62**, 6270 (2000).  
 [8] F. Jasch and A. Blumen, *J. Chem. Phys.* **117**, 2474 (2002).  
 [9] A. Blumen and F. Jasch, *J. Phys. Chem.* **A106**, 2313 (2002).  
 [10] R. Cohen, K. Erez, D. ben-Avraham, and S. Havlin, *Phys. Rev. Lett* **85**, 4626 (2000).  
 [11] R. Cohen, K. Erez, D. ben-Avraham, and S. Havlin, *Phys. Rev. Lett* **86**, 3682 (2001).  
 [12] R. Cohen, D. ben-Avraham, and S. Havlin, *Phys. Rev. E* **66**, 036113 (2002).  
 [13] D. S. Callaway, M. E. J. Newman, S. H. Strogatz, and D. J. Watts, *Phys. Rev. Lett.* **85**, 5468 (2000).  
 [14] K. I. Goh, B. Kahng, and D. Kim, *Phys. Rev. E* **64**, 051903 (2001).  
 [15] I. J. Farkas, I. Derenyi, A.-L. Barabási, and T. Vicsek, *Phys. Rev. E* **64**, 026704 (2001).  
 [16] S. N. Dorogovtsev, A. V. Goltsev, J. F. F. Mendes, and A. N. Samukhin, *Phys. Rev. E* **68**, 046109 (2003).  
 [17] A. Bar-Haim, J. Klafter, and R. Kopelman, *J. Am. Chem. Soc.* **119**, 6197 (1997).  
 [18] R. Kopelman, M. Shortreed, Z.-Y. Shi, W. Tan, Z. Xu, J. S. Moore, A. Bar-Haim, and J. Klafter, *Phys. Rev. Lett.* **78**, 1239 (1997).  
 [19] F. Jasch, C. von Ferber, and A. Blumen, *Phys. Rev. E* **68**, 051106 (2003).  
 [20] K. Broderix, T. Aspelmeier, A. K. Hartmann, and A. Zippelius, *Phys. Rev. E* **64**, 021404 (2001).  
 [21] M. J. Stephen, *Phys. Rev. B* **17**, 4444 (1977).  
 [22] G. J. Rodgers, and A. J. Bray *Phys. Rev. B* **37**, 3557 (1988).  
 [23] K. Broderix, H. Löwe, P. Müller, and A. Zippelius, *Europhys. Lett.* **48**, 421 (1999).  
 [24] K. Broderix, H. Löwe, P. Müller, and A. Zippelius, *Phys. Rev. E* **63**, 011510 (2000).  
 [25] R. B. Stinchcombe, *J. Phys. C* **7**, 179 (1974).  
 [26] P. Biswas, R. Kant, and A. Blumen, *Macromol. Theory Simul.* **9**, 56 (2000).  
 [27] P. Biswas, R. Kant, and A. Blumen, *J. Chem. Phys.* **114**, 2430 (2001).  
 [28] C. von Ferber and A. Blumen, *J. Chem. Phys.* **116**, 8616 (2002).  
 [29] A. Blumen, A. Jurjiu, T. Koslowski, and C. von Ferber, *Phys. Rev. E* **67**, 061103 (2003).  
 [30] A. A. Gurtovenko and A. Blumen, *Macromolecules* **35**, 3288 (2002).  
 [31] M. Molloy and B. Reed, *Random Struct. Algorithms* **6**, 161 (1995).  
 [32] M. Molloy and B. Reed, *Combinatorics, Probab. Comput.* **7**, 295 (1998).  
 [33] M. E. J. Newman, S. H. Strogatz, and D. J. Watts, *Phys. Rev. E* **64**, 026118 (2001).  
 [34] M. E. Fisher and J. W. Essam, *J. Math. Phys.* **2**, 609 (1961).  
 [35] D. Stauffer, *Introduction to Percolation Theory* (Taylor and Francis, London, 1985).  
 [36] M. Mezard, G. Parisi, and M. A. Virasoro, *Spin Glass Theory and Beyond* (World Scientific, Singapore, 1986).  
 [37] P. Bialas and Z. Burda, *Phys. Lett. B* **384**, 75 (1996).  
 [38] W. H. Press, B. P. Flannery, S. A. Teukolsky, and W. T. Vetterling, *Numerical Recipes* (Cambridge University Press, Cambridge, 1990).  
 [39] J. H. Wilkinson and C. Reinsch, *Linear Algebra, Handbook for Automatic Computation, vol. 2* (Springer, New York, 1971).